ATLAS NOTE

ATLAS-CONF-2010-063

July 21, 2010

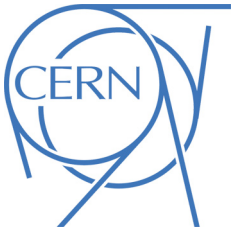

Search for top pair candidate events in ATLAS at $\sqrt{s} = 7$ TeV

The ATLAS Collaboration

Abstract

A search is performed for events consistent with top quark pair production in 280 nb^{-1} of ATLAS pp collision data taken at $\sqrt{s} = 7$ TeV. Several candidate events are observed, in both the lepton plus jets and dilepton topologies. The properties of these events are described, and compared to the expectations from Monte Carlo simulation.

1 Introduction

Assuming an estimated total $t\bar{t}$ production cross section of 160 pb at $\sqrt{s} = 7$ TeV [1], we expect the production of one top quark pair decaying into the e/μ+jets channel for every 20 nb^{-1} of recorded LHC data, as well as one top quark pair decaying into the ee/eμ/$\mu\mu$+jets channel for every 110 nb^{-1} of data.[1] While experimental selection criteria will further reduce the number of observable candidates, a handful of such candidates are expected to be selected with O(100) nb^{-1} of data.

This note describes a search for such candidate events in 280 nb^{-1} of ATLAS pp collision data taken at $\sqrt{s} = 7$ TeV, using an event selection designed for an early measurement of the $t\bar{t}$ production cross-section. The selection is broadly based on that described in [2], but has been re-optimised for $\sqrt{s} = 7$ TeV and uses b-tagging in the lepton plus jets channel. After introducing the data selection and corresponding samples of Monte Carlo simulated data, the object and event selections for both lepton plus jets and dilepton topologies are described. The properties of selected candidate events are discussed, and compared with the expectation from simulation.

2 Data sample

The ATLAS detector [3] covers nearly the entire solid angle around the collision point with layers of tracking detectors, calorimeters and muon chambers.[2] All these detectors play important roles in the reconstruction of $t\bar{t}$ event candidates, and only data where all were fully operational is used. Applying these requirements to $\sqrt{s} = 7$ TeV pp collision data taken in stable beam conditions and recorded up until 19th July 2010 results in a data sample of about 280 nb^{-1}. This luminosity estimate has an uncertainty of 11%[4].

3 Simulated event samples

For the generation of $t\bar{t}$ signal and single top events, MC@NLO [5] v3.41 was used, with PDF set CTEQ66 [6], assuming a top mass of 172.5 GeV and normalizing the $t\bar{t}$ cross-section to the prediction of [1], which is consistent with other NLO calculations. For single top the s, t and Wt channels are included, normalizing to the MC@NLO cross-section and using the 'diagram removal scheme' [7] for Wt to remove overlaps with the $t\bar{t}$ final state.

For the generation of W+($b\bar{b}$)+jets, γ^*/Z+($b\bar{b}$)+jets (Drell-Yan), and QCD multi-jet events, Alpgen v2.13 was used, invoking the MLM matching scheme [8] with matching parameters RCLUS=0.7 and ETCLUS=20, and using parton density function set CTEQ6L1 [9]. For the γ^*/Z+jets the phase space has been restricted to $m(l^+l^-) > 40$ GeV. The W/Z+jets samples were normalized with a K-factor of 1.22 [10]. For the QCD multi-jet sample the generator-level p_T of the leading parton must be at least 35 GeV. QCD multi-jet events have also been subjected to filtering prior to full event simulation: events must have either a truth muon within $|\eta| < 2.8$ with a p_T of at least 10 GeV, or contain at least three truth jets (reconstructed from simulated stable particles after hadronization with the anti-k_t algorithm [11] with parameter R=0.4) with a p_T greater than 25 GeV, as well as an additional truth jet with a p_T greater than 17 GeV. [3] The QCD samples were normalized using the Alpgen prediction. All events were

[1] The values include small contributions from $\tau \to e$ and $\tau \to \mu$ decays.

[2] In the right-handed ATLAS coordinate system, the pseudorapidity η is defined as $\eta = -\ln(\tan(\theta/2))$, where the polar angle θ is measured with respect to the LHC beamline. The azimuthal angle ϕ is measured with respect to the x-axis, which points towards the centre of the LHC ring. The z-axis is parallel to anti-clockwise beam.

[3] For the electron plus jets channel, these filter cuts are slightly tighter than the final analysis cuts, however the magnitude of this effect has been calculated to be about 10 %, which is small in comparison with the expected total uncertainty on the QCD background rate after selection.

hadronized with Herwig [12], using Jimmy [13] for the underlying event model. Diboson WW, WZ and ZZ+jet events were produced using Herwig, normalized as in [10]. The effect of pileup, *i.e.* additional proton-proton interactions in the same beam crossing, was not simulated.

Subsequent detector and trigger simulation, followed by offline reconstruction, has been performed with standard ATLAS software making use of GEANT4 [14].

4 Object selection

The reconstruction of $t\bar{t}$ events makes use of reconstructed electrons, muons and jets, and the overall momentum balance in the transverse plane. The following criteria are used to define the selected objects in the events:

- *Electrons:* Electron candidates are required to pass the medium electron selection as defined in [15], with $p_T > 20$ GeV and $|\eta_{cluster}| < 2.47$, excluding the calorimeter crack region at $1.37 < |\eta_{cluster}| < 1.52$, where $\eta_{cluster}$ is the pseudo-rapidity of the calorimeter energy cluster associated with the candidate. In addition, the track must have an associated hit in the innermost pixel layer in order to remove photon conversions (except in regions with known dead modules), and the energy deposition in the calorimeter within a cone of radius $\Delta R = 0.2$ must be less that $4\text{ GeV} + 0.023 \cdot p_T^{\ell}$, where $\Delta R = \sqrt{\Delta\eta^2 + \Delta\phi^2}$ and p_T^{ℓ} is the transverse momentum of the lepton. The last requirement ensures electrons are isolated, reducing the rate of hadrons in jets misidentified as electrons, and suppressing the selection of electrons from heavy flavour decays inside jets.

- *Muons:* Muons are reconstructed by combining muon tracks from the inner detector and muon spectrometer, as defined as 'chain 2' in [16], with $p_T > 20$ GeV and $|\eta| < 2.5$. To ensure isolation, the energy deposition in the calorimeter and the sum of track transverse momenta measured in cones of radius of $\Delta R = 0.3$ around the muon track are each required to be less than 4 GeV. Additionally, muons are required to have a distance ΔR greater than 0.4 from any jet with $p_T > 20$ GeV, further suppressing muons from heavy flavour decays inside jets.

- *Jets:* Jets are reconstructed with the anti-k_t algorithm (R=0.4) clustered from EM-scale topological clusters in the calorimeters [17]. These jets are then calibrated to the hadronic energy scale, using a p_T and η dependent correction factor obtained from simulation [18]. If a jet is the closest jet to an electron candidate and the corresponding distance ΔR is less than 0.2, the jet is removed from consideration in order to avoid double-counting of electrons as jets. Jets are considered b-tagged if the secondary vertex-based tagger SV0 returns a value above a threshold that is defined by a 50% tagging efficiency, obtained from studies of simulated $t\bar{t}$ events [19].

- *Missing transverse energy:* The missing transverse energy is constructed from the vector sum of all calorimeter cells, resolved into the transverse plane. Cells not associated to a jet or electron are included at the EM scale. Cells associated with jets are taken at the corrected energy scale that was used for jets, while the contribution from cells associated with electrons are substituted by the calibrated transverse energy of the electron. Finally, the contribution from muons passing the 'chain 2' requirements are included, also removing the contribution of any calorimeter cell associated to the muon.

5 Event selections

The selections for both lepton+jets and dilepton events start by requiring the presence of at least one lepton (e or μ) associated with a leptonic high-level trigger object of the same flavour with a 10 GeV p_T

threshold. Events must have a reconstructed primary vertex with at least 5 tracks, and are discarded if any jet with $p_T > 10$ GeV at the EM scale fails jet quality cuts designed to reject jets arising from out-of-time activity or calorimeter noise [20]. These quality cuts remove a negligible fraction of simulated events.

The lepton+jets selection then requires the presence of exactly one offline-reconstructed electron or muon with $p_T > 20$ GeV, satisfying the object requirements given in Section 4 above and matching a leptonic high-level trigger object within $\Delta R < 0.15$. At least four jets with $p_T > 20$ GeV and $|\eta| < 2.5$ are then required, at least one of which must be b-tagged. Finally, the missing transverse energy must satisfy $E_{\mathrm{T}}^{\mathrm{miss}} > 20$ GeV.

The dilepton selection requires two oppositely-charged leptons (ee, $\mu\mu$ or $e\mu$) each satisfying $p_T > 20$ GeV, at least one of which must be associated to a leptonic high-level trigger object. At least two jets with $p_T > 20$ GeV are required, but no b-tagging requirements are imposed. In the ee channel, to suppress backgrounds from Drell-Yan and QCD multi-jet events, the missing transverse energy must satisfy $E_{\mathrm{T}}^{\mathrm{miss}} > 40$ GeV, and the invariant mass of the two leptons must be at least 5 GeV from the Z-boson mass, *i.e.* $|m_{ee} - m_Z| > 5$ GeV. For the muon channel, the corresponding requirements are $E_{\mathrm{T}}^{\mathrm{miss}} > 30$ GeV and $|m_{\mu\mu} - m_Z| > 10$ GeV. For the $e\mu$ channel, where the background from $Z \to ee$ and $Z \to \mu\mu$ is expected to be much smaller, no $E_{\mathrm{T}}^{\mathrm{miss}}$ or Z-mass veto cuts are applied, but the event H_{T}, defined as the scalar sum of the transverse energies of the two leptons and all the selected jets, must satisfy $H_{\mathrm{T}} > 150$ GeV.

6 Candidate events and distributions

Tables 1 and 2 list events found in data that pass all event selection criteria in the lepton plus jets and dilepton channels, and tabulate some of the basic properties of these events. For the lepton plus jets candidates, the transverse mass m_T of the lepton-$E_{\mathrm{T}}^{\mathrm{miss}}$ system is calculated as described in [15]. The distribution of m_T for events containing a leptonic W decay is peaked at the W boson mass with a tail down to about 40 GeV, whereas events without a leptonic W decay predominantly have m_T values much lower than 40 GeV. The three-jet mass m_{jjj} is defined as the invariant mass of the three-jet combination with the largest p_T, and provides an approximate estimate of the mass of the hadronically-decaying top quark.

ID	Run number	Event number	Channel	p_T^{lep} (GeV)	$E_{\mathrm{T}}^{\mathrm{miss}}$ (GeV)	m_T (GeV)	m_{jjj} (GeV)	#jets $p_T > 20$ GeV	#b-tagged jets
LJ1	158801	4645054	μ+jets	42.9	25.1	59.3	314	7	1
LJ2	158975	21437359	e+jets	41.4	89.3	68.7	106	4	1
LJ3	159086	12916278	e+jets	26.2	46.1	62.6	94	4	1
LJ4	159086	60469005	e+jets	39.1	66.7	102	231	4	1
LJ5	159086	64558586	e+jets	79.3	43.4	86.7	122	4	1
LJ6	159224	13396261	μ+jets	29.4	65.4	64.1	126	5	1
LJ7	159224	13560451	μ+jets	78.7	40.0	83.7	108	4	1

Table 1: List of candidate $t\bar{t}$ events in the lepton+jets channel in data, showing the ID used in the text, the run and event numbers, channel, lepton p_T, missing transverse energy $E_{\mathrm{T}}^{\mathrm{miss}}$, transverse mass m_T, reconstructed 3-jet mass m_{jjj}, total number of selected jets and number of b-tagged jets.

Some of the event properties are also indicated as arrows in the corresponding distributions on Figures 1 to 7. The Monte Carlo simulation distributions on these plots show the expected relative contributions of the various signal and background processes discussed in Section 3. Only events passing all selection cuts are shown, and each plot is normalized so that the sum of all expected processes is unity.

ID	Run number	Event number	Channel	p_T^{lep} (GeV)	$E_{\mathrm{T}}^{\mathrm{miss}}$ (GeV)	H_T (GeV)	#jets $p_T > 20$ GeV	#b-tagged jets
DL1	155678	13304729	ee	55.2/40.6	42.4	271	3	1
DL2	158582	27400066	$e\mu$	22.7/47.8	76.9	196	3	1

Table 2: List of candidate $t\bar{t}$ events in the dilepton channel in data, showing the ID used in the text, the run and event numbers, channel, lepton p_T values, missing transverse energy $E_{\mathrm{T}}^{\mathrm{miss}}$, energy sum H_{T}, total number of selected jets and number of b-tagged jets.

Figure 1 shows the three-jet mass m_{jjj} distributions for the electron+jets (left) and muon+jets (right) selections, and Figure 2 the corresponding $E_{\mathrm{T}}^{\mathrm{miss}}$ distributions. It should be noted that the simulated event sample for the QCD multi-jet background has significantly lower integrated luminosity than the others, and suffers from large intrinsic uncertainties due to limited knowledge of the production cross section and the probabilities that jets are mis-identified as leptons. A full quantitative evaluation of this background requires further study in data samples larger than those presently available.

For the ee dilepton selection, Figure 3 shows the number of selected jets with $p_T > 20$ GeV, and the number of b-tagged jets. Figures 4 and 5 show the corresponding distributions for $\mu\mu$ and $e\mu$ events. Figure 6 shows the $E_{\mathrm{T}}^{\mathrm{miss}}$ distributions for the ee and $\mu\mu$ channels, and Figure 7 the H_{T} distribution for the $e\mu$ channel. No QCD multi-jet background events are shown in the dilepton channel as none pass the selection criteria.

6.1 Comments on selected candidate events

- Candidate LJ1 - The missing transverse energy of this candidate is aligned with one of the jets in the event, which makes it more likely that the event stems from a background process.
- Candidates LJ3 and LJ5 - In addition to the jet tagged with the SV0 algorithm, both these events have a second jet tagged as a b-jet by the JetProb and TrackCounting algorithms [21] at 50%-efficiency working points, but not by the SV0 tagger which is used in the analysis.
- Candidate DL1 - The invariant mass of the two electron candidates is 36.9 GeV.
- Candidate DL2 - This event has a second primary vertex from a pileup collision. However all leptons and jets considered for the top analysis are associated with a single vertex in this event.

6.2 Event displays of selected candidates

Figures 8, 9 and 10 show event displays for candidates LJ2, DL1 and DL2. Further details of the interpretation are given in the figure captions.

7 Conclusion

A search for candidate events consistent with the production of top quark pairs was conducted using a $280\,\mathrm{nb}^{-1}$ sample of pp collision data collected with the ATLAS detector at $\sqrt{s} = 7$ TeV. Using an event selection designed for an early measurement of the $t\bar{t}$ cross-section, and the present understanding of the ATLAS detector performance and data quality, 9 candidate events were seen, comprising 4 e plus jets, 3 μ plus jets, 1 ee, 0 $\mu\mu$ and 1 $e\mu$ dilepton events. These events counts are consistent with expectations from simulation; specifically no channel count in data exceeds the simulation prediction with a Poisson probability of less than 20 %.

Kinematic properties of these events are consistent with $t\bar{t}$ production. Although events are observed in regions where the $t\bar{t}$ purities expected from simulation studies are high, larger data samples and further studies of data in control regions will be required to quantify the background to a level where it can support a conclusive statement on the observation of top quark production in ATLAS.

References

[1] S. Moch and P. Uwer, Theoretical status and prospects for top-quark pair production at hadron colliders, Phys. Rev. D78 (2008) 034003, arXiv:0804.1476 [hep-ph];
U. Langenfeld, S. Moch, and P. Uwer, New results for ttbar production at hadron colliders, arXiv:0907.2527 [hep-ph].

[2] The ATLAS Collaboration, Prospects for measuring top pair production in the dilepton channel with early ATLAS data at $\sqrt{s}$ = 10 TeV, ATL-PHYS-PUB-2009-086;
The ATLAS Collaboration, prospects for the Top Pair Production Cross-section at $\sqrt{s}$ = 10 TeV in the Single Lepton Channel in ATLAS, ATL-PHYS-PUB-2009-087.

[3] G. Aad et al., ATLAS Collaboration, JINST 3 S08003 (2008).

[4] The ATLAS Collaboration, Luminosity Determination Using the ATLAS Detector, ATLAS-CONF-2010-60.

[5] S. Frixione and B.R. Webber, Matching NLO QCD computations and parton shower simulations, JHEP 06 (2002) 029, arXiv:hep-ph/0204244;
S. Frixione, P. Nason and B.R. Webber, Matching NLO QCD and parton showers in heavy flavour production, JHEP 08 (2003) 007, arXiv:hep-ph/0305252;
S. Frixione, E. Laenen and P. Motylinski, Single-top production in MC@NLO, JHEP 03 (2006) 092, arXiv:hep-ph/0512250.

[6] P.M. Nadolsky et al., Implications of CTEQ global analysis for collider observables, Phys. Rev. D78 (2008) 013004, arXiv:0802.0007 [hep-ph].

[7] S. Frixione, E. Laenen, P. Motylinski, B.R. Webber and C.D. White, Single-top hadroproduction in association with a W boson, JHEP 07 (2008) 029, arXiv:0805.3067 [hep-ph].

[8] M. L. Mangano, M. Moretti, F. Piccinini, R. Pittau and A.D. Polosa, ALPGEN, a generator for hard multiparton processes in hadronic collisions, JHEP 07 (2003) 001, arXiv:hep-ph/0206293.

[9] J. Pumplin et al., New generation of parton distributions with uncertainties from global QCD analysis, JHEP 07 (2002) 012, arXiv:hep-ph/0201195.

[10] The ATLAS Collaboration, Expected Performance of the ATLAS Experiment: Detector, Trigger and Physics, CERN-OPEN-2008-020, pages 874–878.

[11] M. Cacciari, G.P. Salam and G. Soyez, JHEP 0804 (2008) 063.

[12] G. Corcella et al., HERWIG 6.5: an event generator for Hadron Emission Reactions With Interfering Gluons (including supersymmetric processes), JHEP 01 (2001) 010, arXiv:hep-ph/0011363;
G. Corcella et al., HERWIG 6.5 release notes, arXiv:hep-ph/0210213.

[13] Multiparton interactions in photoproduction at HERA, J.M. Butterworth et al., Z. Phys. C72 (1996) 637.

[14] S. Agostinelli et al., Geant4 – a simulation toolkit, Nucl. Instr Meth. A 506 (2003) 250;
J. Allison et al., Geant4 developments and applications, IEEE Transactions on Nuclear Science 53 No. 1 (2006) 270–278.

[15] The ATLAS Collaboration, Observation of $W \to \ell\nu$ and $Z \to \ell\ell$ production in proton-proton collisions at $\sqrt{s}$ = 7 TeV with the ATLAS detector, ATLAS-CONF-2010-044.

[16] The ATLAS Collaboration, Muon Performance in Minimum Bias pp Collision Data at $\sqrt{s}$ = 7 TeV with ATLAS, ATLAS-CONF-2010-036.

[17] The ATLAS Collaboration, Properties of Jets and Inputs to Jet Reconstruction and Calibration with the ATLAS Detector using Proton-Proton Collisions at $\sqrt{s}$ = 7 TeV, ATLAS-CONF-2010-053.

[18] The ATLAS Collaboration, Jet energy scale and its systematic uncertainty in ATLAS for jets produced in proton-proton collisions at $\sqrt{s}$ =7 TeV, ATLAS-CONF-2010-056.

[19] The ATLAS Collaboration, Performance of the ATLAS Secondary Vertex b-tagging Algorithm in 7 TeV Collision Data, ATLAS-CONF-2010-042.

[20] The ATLAS Collaboration, Data-Quality Requirements and Event Cleaning for Jets and Missing Transverse Energy Reconstruction with the ATLAS Detector in Proton-Proton Collisions at a Center-of-Mass Energy of $\sqrt{s}$ = 7 TeV, ATLAS-CONF-2010-038.

[21] The ATLAS Collaboration, Impact parameter-based b-tagging algorithms in the 7 TeV collision data with the ATLAS detector: the TrackCounting and JetProb algorithms, ATLAS-CONF-2010-041.

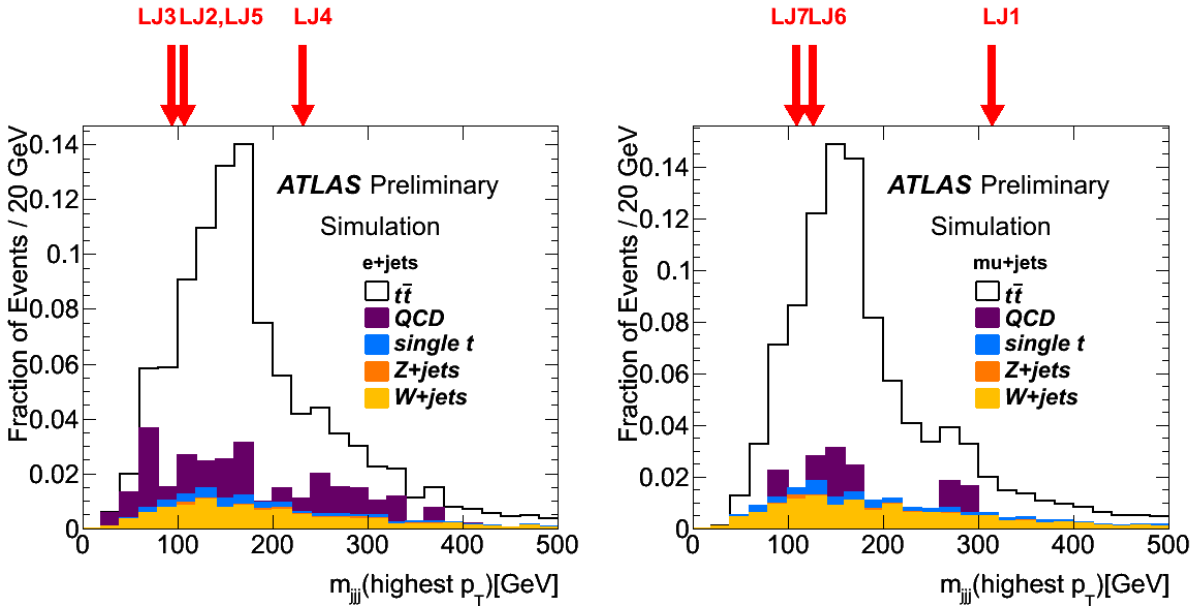

Figure 1: Distributions of m_{jjj}, the invariant mass of the 3-jet combination having the highest p_T, for events passing the electron plus jets (left) and muon plus jets (right) selections. In this and the following figures, the positions of data candidate events are indicated by arrows.

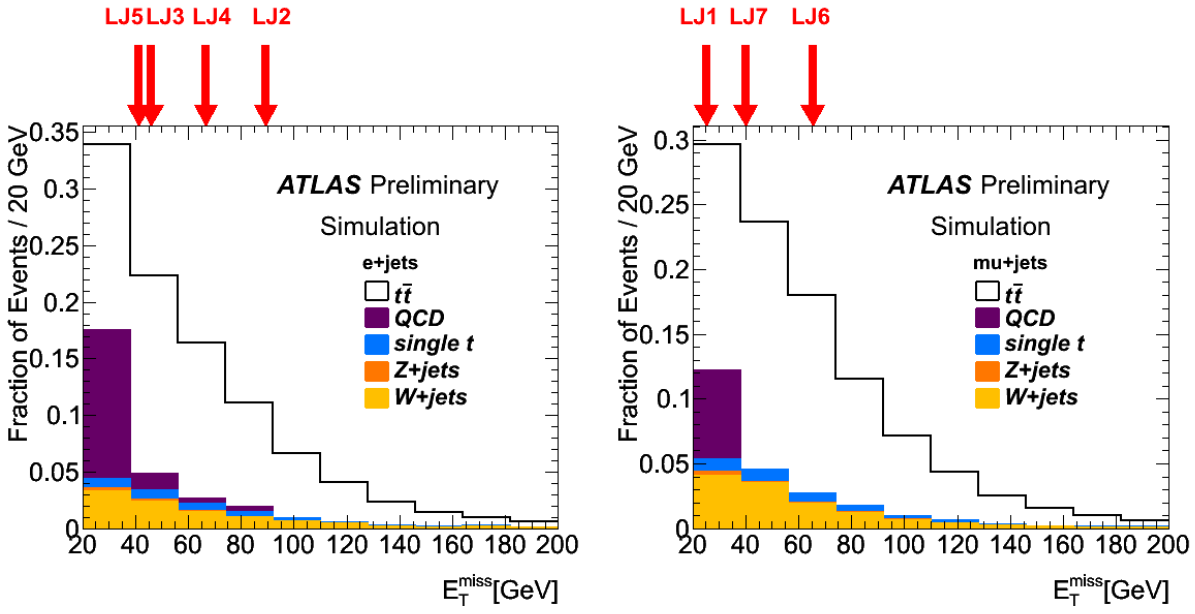

Figure 2: Distributions of $E_{\mathrm{T}}^{\mathrm{miss}}$ for events passing the electron plus jets (left) and muon plus jets (right) selections.

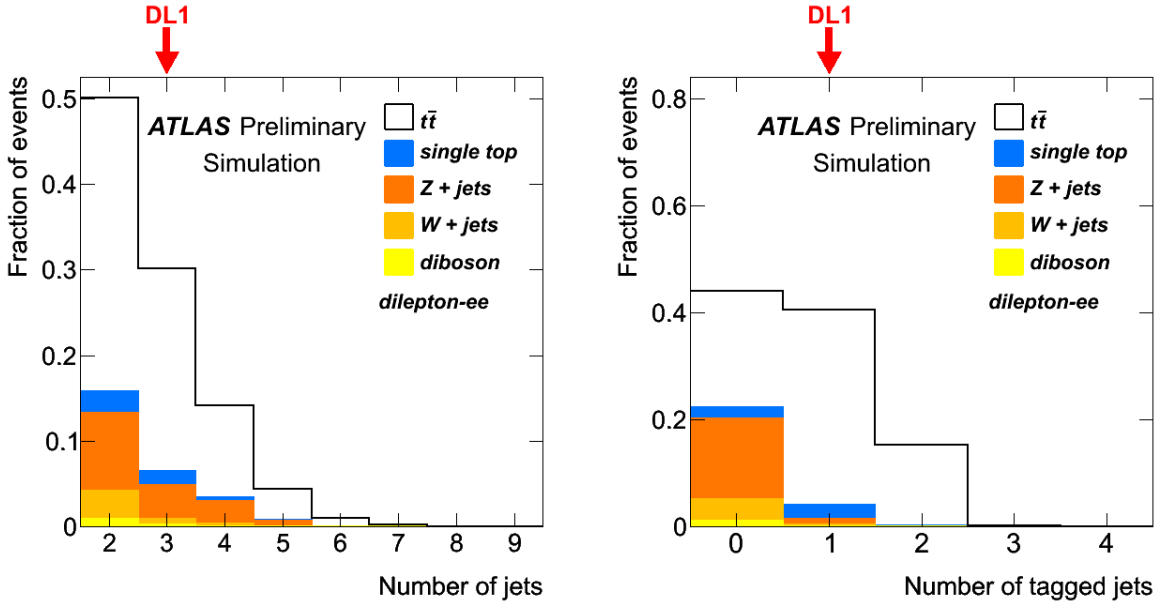

Figure 3: Distributions of the number of jets, and the number of b-tagged jets, for events passing the ee dilepton event selection.

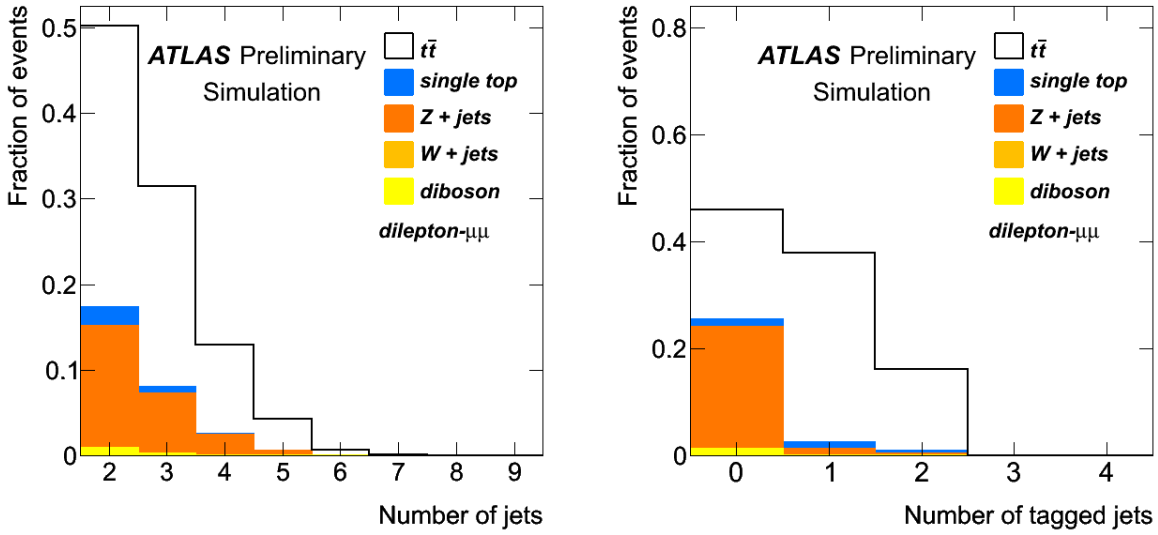

Figure 4: Distributions of the number of jets, and the number of b-tagged jets, for events passing the $\mu\mu$ dilepton event selection.

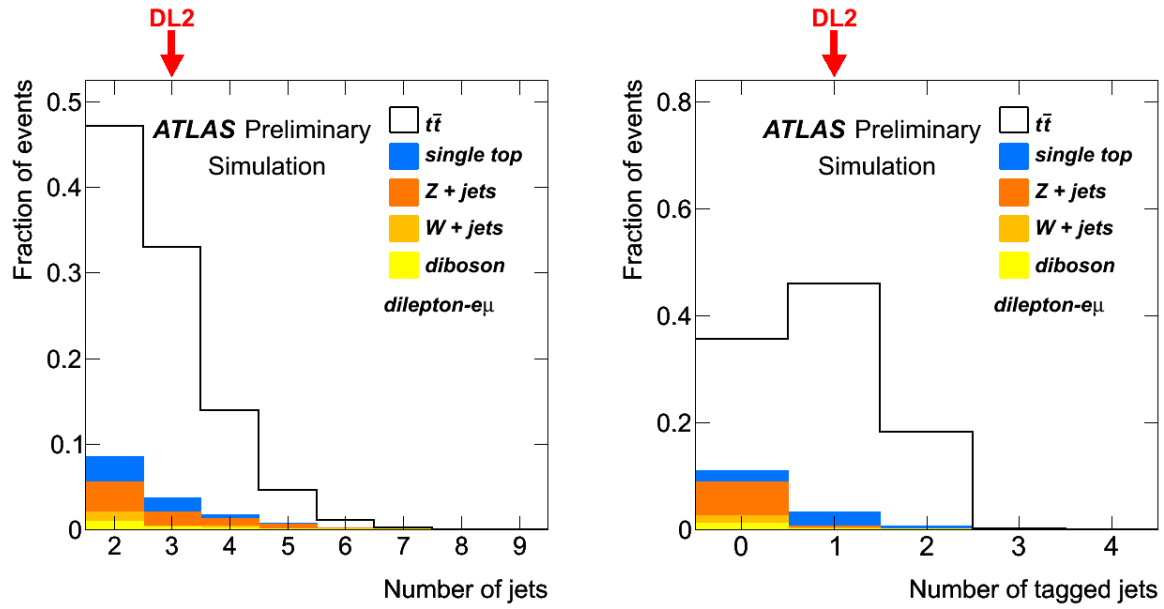

Figure 5: Distributions of the number of jets, and the number of b-tagged jets, for events passing the $e\mu$ dilepton event selection.

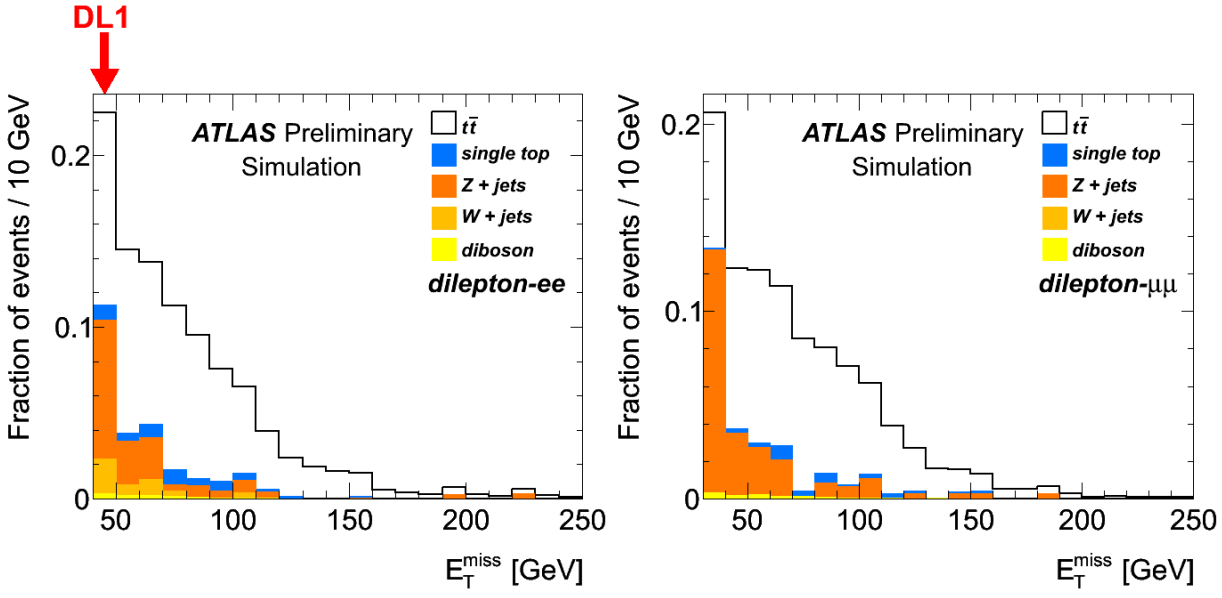

Figure 6: Distributions of $E_{\mathrm{T}}^{\mathrm{miss}}$ for events passing the ee and $\mu\mu$ dilepton event selections.

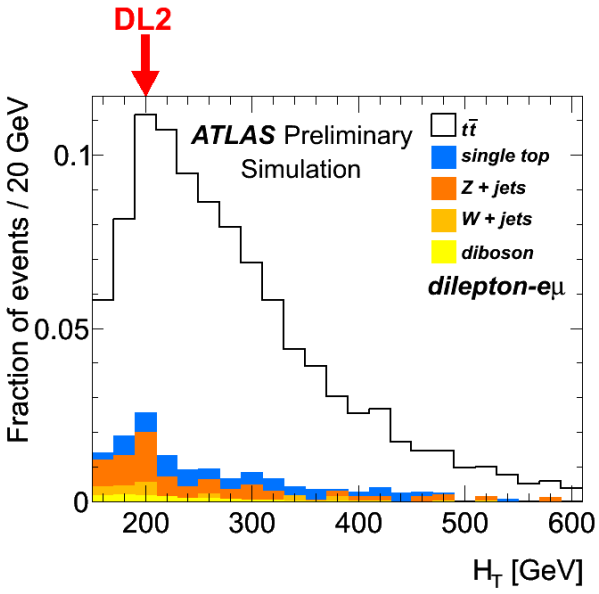

Figure 7: Distribution of H_{T} for events passing the $e\mu$ dilepton event selection.

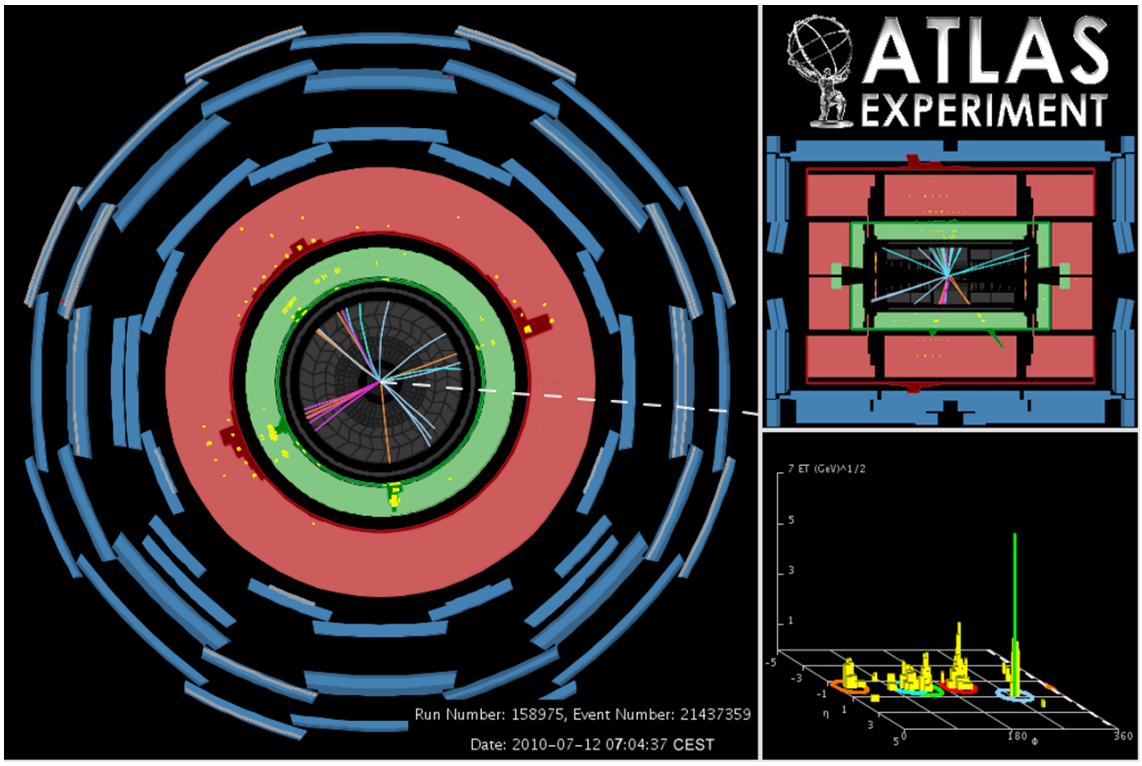

Figure 8: Event display of the electron plus jets candidate LJ2. The electron is shown as the orange downward-pointing track associated to the green cluster, and as the green tower in the η-ϕ lego plot. The direction of the missing transverse energy is shown as the dotted line in the r-ϕ view.

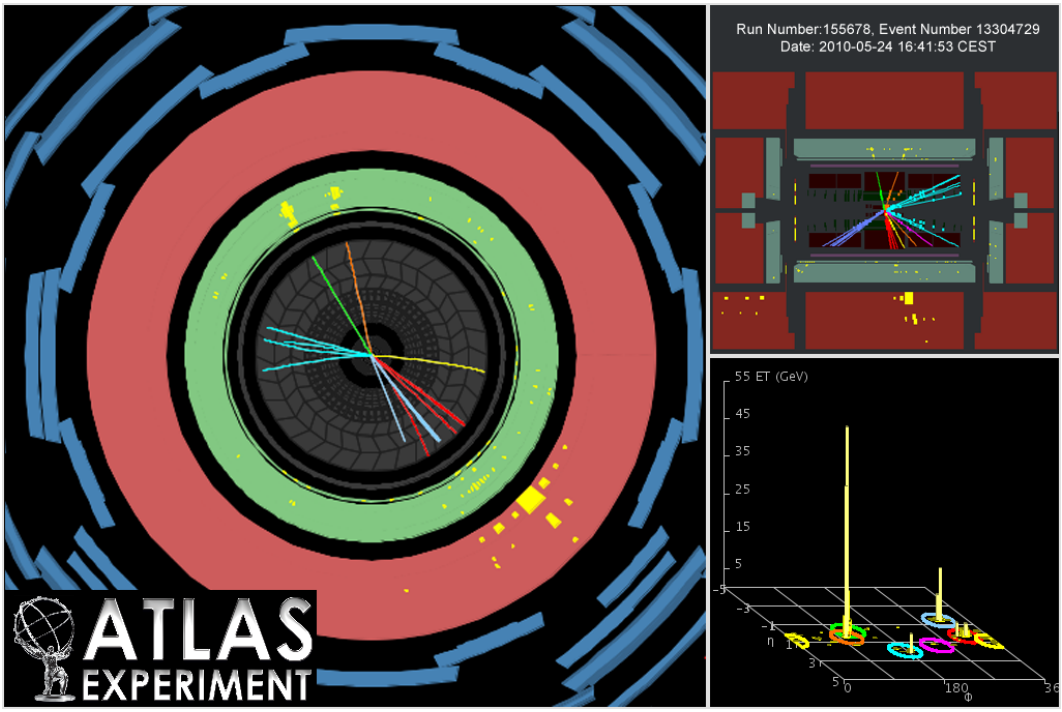

Figure 9: Event display of the *ee* dilepton candidate DL1. The electrons are shown as the two upward-pointing orange and green tracks.

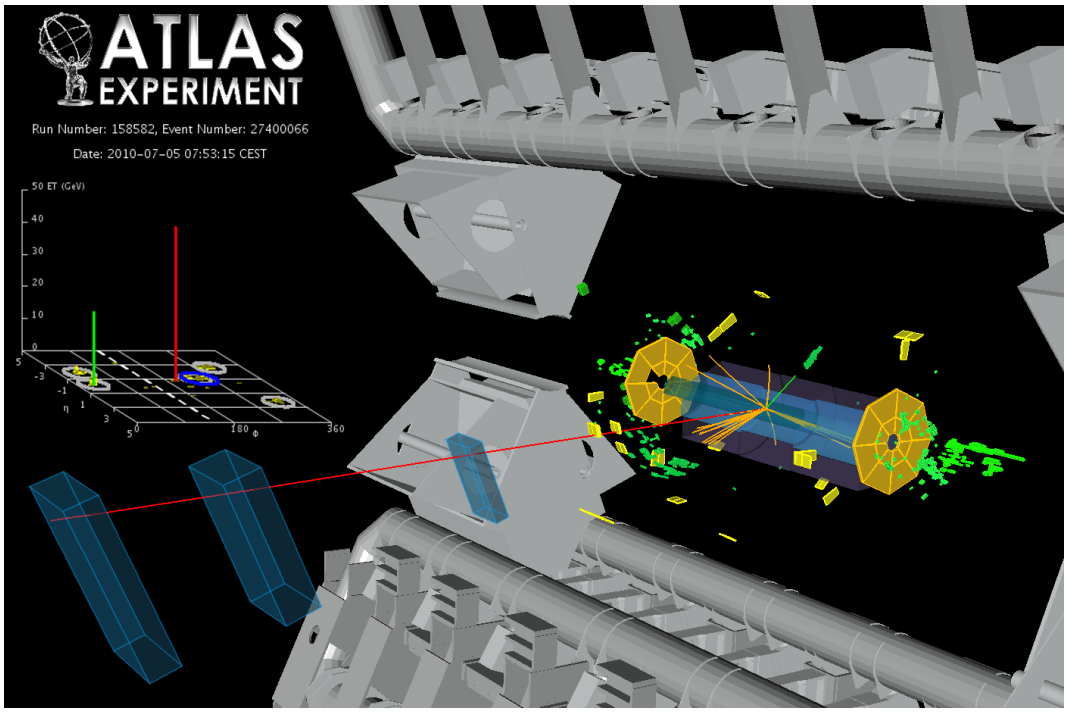

Figure 10: Event display of the $e\mu$ dilepton candidate DL2. The isolated muon track is shown in red, the isolated electron is shown as a green track pointing to a green cluster. The b-tagged jet is marked as a blue circle in the $\eta - \phi$ lego plot. The direction of the missing transverse energy is shown as a dashed line in the $\eta - \phi$ lego plot.